

## Supplementary Material

### *White matter CBF correction for global CBF estimates for a single-compartment kinetic model*

Simulations were performed to address the effect on white matter (WM) CBF quantification when using parameters for WM, tissue  $T_{1,WM}$  and arterial (bolus) arrival time,  $BAT_{WM}$  instead of gray matter (GM) tissue  $T_{1,GM}$  and  $BAT_{GM}$  in the ASL CBF quantification model as commonly done.

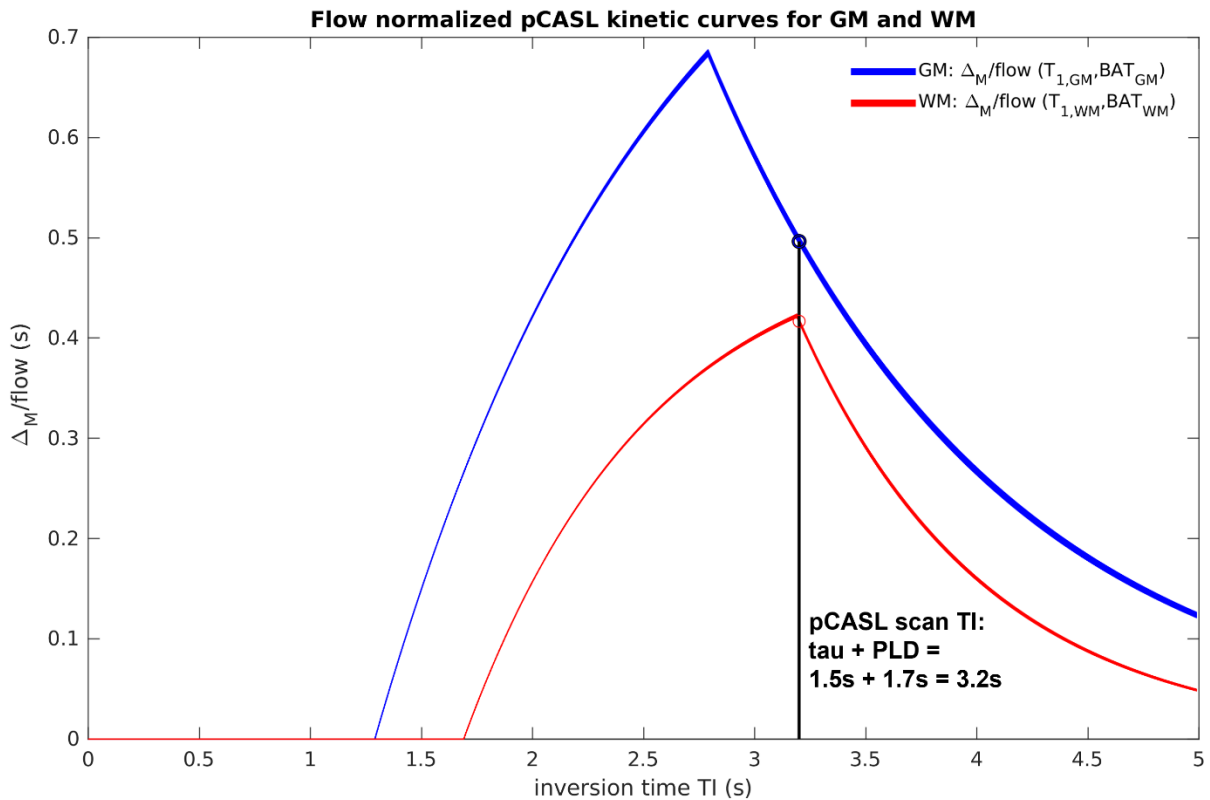
The conversion of pCASL measured  $\Delta M$  to CBF can be considered as a scaling problem, when applying a single-compartment kinetic model (Buxton et al.<sup>1</sup>). Here, the scaling factor 'C' depends on the familiar tissue-specific parameters:  $T_1$  and BAT and 'global' parameters: blood  $T_{1,a}$ , bolus duration  $\tau$ , inversion efficiency  $\alpha$ , blood/tissue water partition coefficient  $\lambda$ , and the voxel specific calibration  $M_{0,b}$ .

Note that the apparent  $T_1'$  dependency on CBF ( $1/T_1' = 1/T_{1,tissue} + f/\lambda$  with  $f = CBF$  in mL/g/s) in the kinetic model makes it deviate from a pure scaling problem, however, the effect of CBF on the apparent  $T_1$  is negligible. The latter can be seen by the very slight broadening of the CBF normalized kinetic curve for different simulated CBF values with respect to inversion time TI (see Supplemental Figure 2 below).

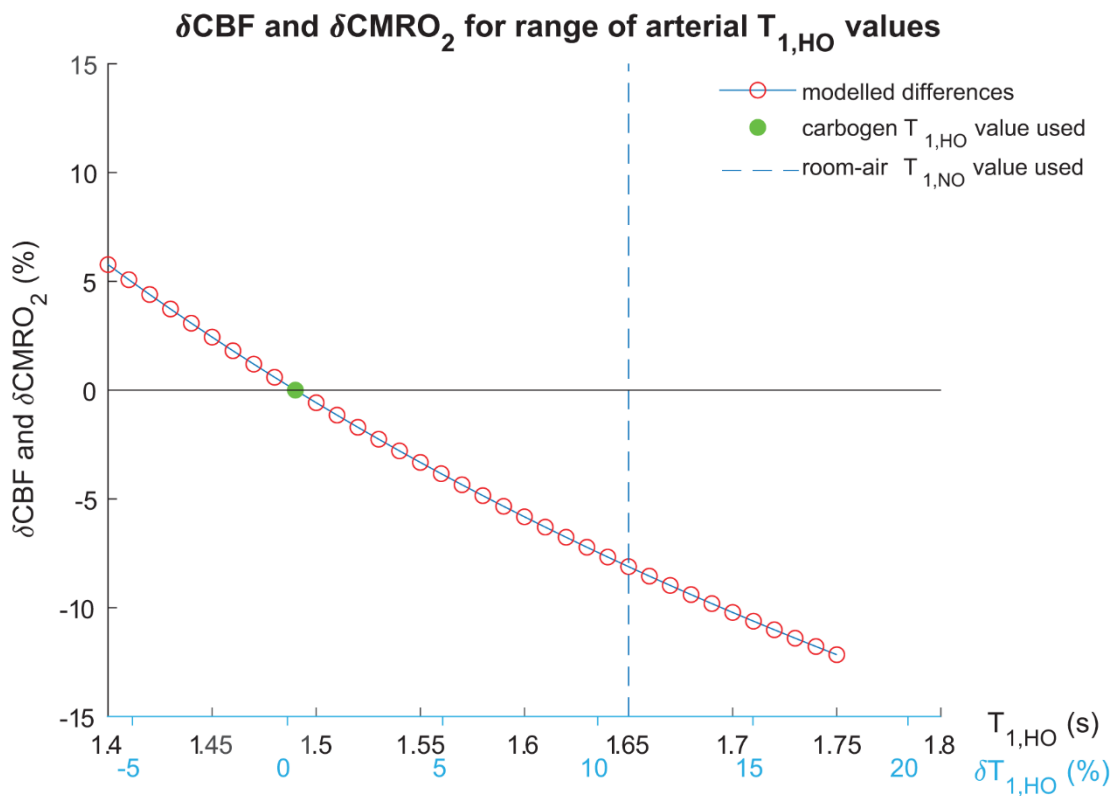
A range of kinetic curves was generated for a range of CBF values ( $0 - 1.5$  ml/g/s  $\cong 0 - 90$  mL/100 g/min) and subsequently normalized by the CBF value. Tissue specific values where  $T_{1,GM} = 1.3s^2$ ,  $T_{1,WM} = 0.84s^2$ ,  $BAT_{GM}^3$  and  $BAT_{WM}^3$ .

The resulting, 'normalized kinetic curves', give the conversion from CBF to  $\Delta M$  with respect to the inversion time TI. The scaling factor C, used to convert  $\Delta M$  to CBF, is then obtained by taking the reciprocal of the normalized kinetic curve at the pCASL sequence's TI. In Supplemental Figure 2 below, CBF normalized kinetic curves for GM and WM based values, tissue  $T_1$  and BAT, are depicted in blue and red, respectively. To convert measured  $\Delta M$  to CBF (in mL/g/s) using GM based values one gets a scaling factor of  $C_{GM} \approx 1/0.5 \approx 2$  for the pCASL sequence inversion time used here:  $TI = \tau + PLD = 1.5s + 1.7s = 3.2s$ . To convert measured  $\Delta M$  to CBF using white matter based values, one gets a scaling factor of  $C_{WM} \approx 1/0.42 \approx 2.4$  at the same inversion time.

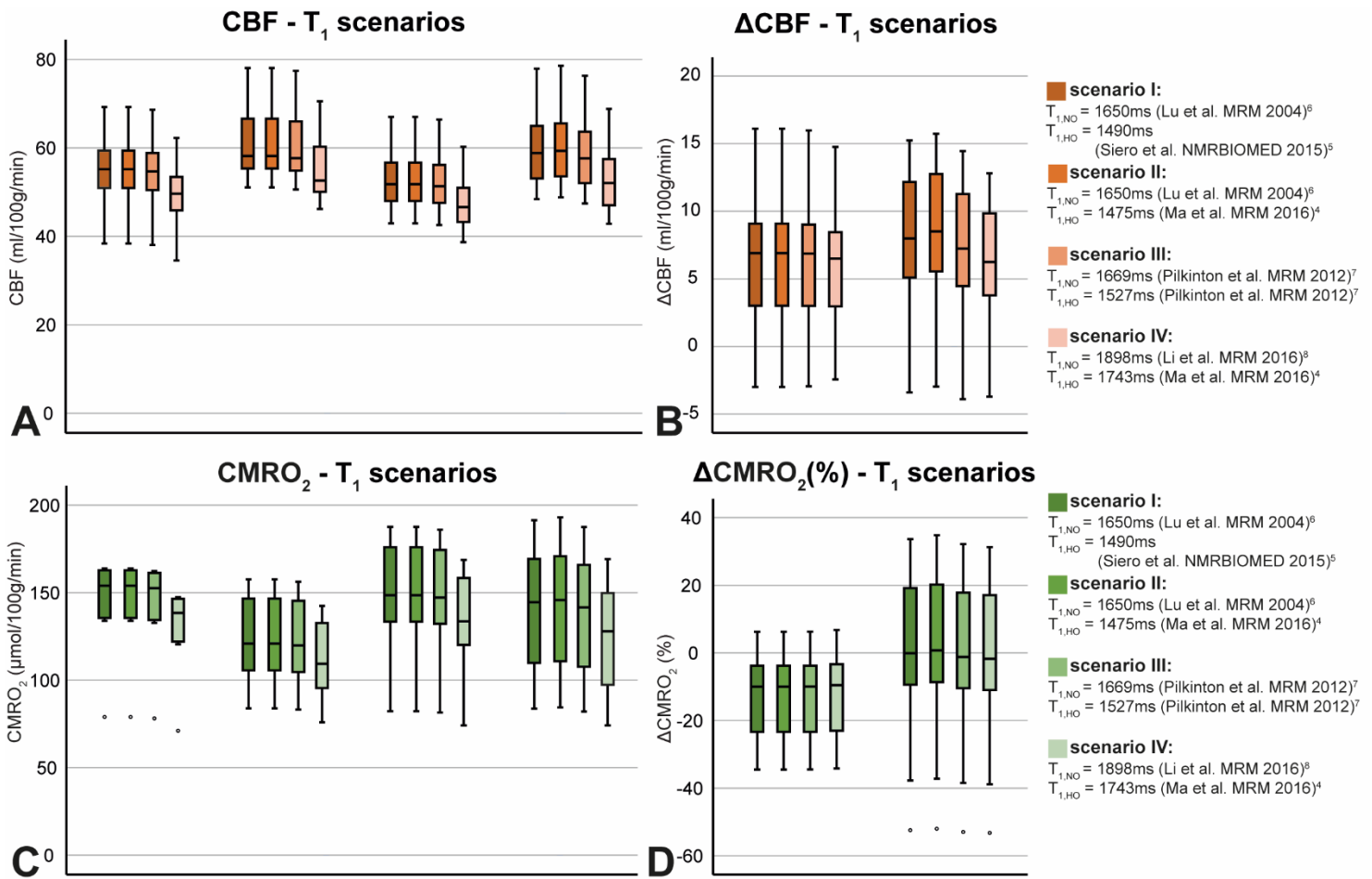
From this exercise, we observe that for WM regions, when using GM based values in CBF quantification, the  $CBF_{WM}$  is underestimated by a factor of  $C_{WM}/C_{GM} \approx 2.4/2 \approx 1.2$ , which is about 20%. This factor can be used to correct the CBF values in the WM ROI, i.e. increasing WM CBF by ~20%, yielding corrected global (whole-brain) CBF estimates and thus  $CMRO_2$  estimates. We found that the  $CMRO_2$  findings did not change notably when incorporating the WM correction on global CBF, the numerical values did change.



**Supplementary Figure 1:** Flow (CBF) normalized kinetic curves for GM and WM based values (tissue T1 and bolus arrival time, BAT) are depicted in blue and red, respectively. These curves give the conversion from CBF to  $\Delta M$  with respect to the inversion time TI. The scaling factor C, to convert  $\Delta M$  to CBF, is then obtained by taking the reciprocal of the normalized kinetic curve at the pCASL sequence's TI. To convert measured  $\Delta M$  to CBF (in mL/g/s) using GM based values one gets a scaling factor of  $C_{GM} \approx 1/0.5 \approx 2$  for the pCASL sequence inversion time used here:  $\text{TI} = \tau + \text{PLD} = 1.5\text{s} + 1.7\text{s} = 3.2\text{s}$ . To convert measured  $\Delta M$  to CBF using white matter based values, one gets a scaling factor of  $C_{WM} \approx 1/0.42 \approx 2.4$  at the same inversion time. As a result, when using GM based values in CBF quantification, the WM CBF is underestimated by a factor of  $C_{WM}/C_{GM} \approx 2.4/2 \approx 1.2$ , which is about 20%. This factor can be used to correct the CBF values in the WM ROI, i.e. increasing WM CBF by  $\sim 20\%$ , yielding corrected global (whole-brain) CBF estimates and thus  $\text{CMRO}_2$  estimates.



**Supplementary Figure 2.** Sensitivity analysis of the effect on hyperoxic arterial blood water T<sub>1,HO</sub> on CBF and CMRO<sub>2</sub> quantification. The T<sub>1,HO</sub> value used for carbogen (1.49s) and variations therein ( $\delta$ ) were plotted against the modelled percentage change ( $\delta$ ) in CBF and CMRO<sub>2</sub> quantification. The used T<sub>1,NO</sub> for room-air (1.65s) is depicted by the dashed blue line. Note CBF and CMRO<sub>2</sub> are directly proportional by the arteriovenous O<sub>2</sub> difference. The resulting percentage change in CBF and CMRO<sub>2</sub> were plotted for a range of possible T<sub>1,HO</sub> values, for absolute values and the percentage difference with respect to the reference T<sub>1,HO</sub> (=1.65s) for carbogen. CBF = cerebral blood flow; CMRO<sub>2</sub> = cerebral metabolic rate of oxygen, T<sub>1,HO</sub> = arterial blood water T<sub>1a</sub> during hyperoxia, T<sub>1,NO</sub> = arterial blood water T<sub>1a</sub> during normoxia.



**Supplementary Figure 3. A) CBF, B)  $\Delta$ CBF, C)  $CMRO_2$  and D)  $\Delta$  $CMRO_2$  results for different arterial blood water  $T_{1a}$  scenarios for normoxic ( $T_{1,NO}$ ) and hyperoxic ( $T_{1,HO}$ ) conditions. Although the absolute CBF and  $CMRO_2$  results change in value, the impact on the  $\Delta$ CBF and notably the  $\Delta$  $CMRO_2$  changes, which is the topic of this study, did not change significantly for the different  $T_1$  scenarios. For the hyperoxic (carbogen) condition, a  $p_aO_2$  of 460 mmHg was assumed, and for scenarios II and IV we incorporated the reported hyperoxic  $T_{1a}$  relativity by Ma et al.<sup>4</sup> (see Methods ‘Effect of arterial blood water  $T_{1a}$  on CBF and  $CMRO_2$  quantification’. CBF = cerebral blood flow;  $CMRO_2$  = cerebral metabolic rate of oxygen;  $p_aO_2$  = partial pressure of arterial  $O_2$ ,  $T_{1,HO}$  = arterial blood water  $T_{1a}$  during hyperoxia,  $T_{1,NO}$  = arterial blood water  $T_{1a}$  during normoxia. The boxplots show the minimum, maximum, median and interquartile range, open circles denote outliers.**

**Supplementary Table 1. Cerebral blood flow (CBF) in gray matter, venous oxygenation ( $Y_v$ ), oxygen extraction fraction (OEF), and cerebral metabolic rate of oxygen ( $CMRO_2$ ) results for the room air, ‘ $CO_2$  in air’ and carbogen breathing conditions for all subjects.**

subj. nr	cerebral blood flow CBF (ml/100g/min)				venous oxygenation $Y_v$ (%)				oxygen extraction fraction OEF				cerebral metabolic rate of $O_2$ $CMRO_2$ ( $\mu$ mol/100g/min)			
	room-air1	$CO_2$ in air	room-air2	carbogen	room-air1	$CO_2$ in air	room-air2	carbogen	room-air1	$CO_2$ in air	room-air2	carbogen	room-air1	$CO_2$ in air	room-air2	carbogen
1	59.35	67.66	42.94	57.75	70.00	79.00	68.00	84.50	0.29	0.19	0.31	0.20	143.05	108.43	111.53	107.56
2	51.34	55.33	49.58	59.46	68.00	71.00	67.00	73.50	0.31	0.28	0.32	0.31	133.92	128.93	133.46	169.33
3	50.94	51.04	48.00	53.09	63.00	72.50	64.00	73.00	0.36	0.26	0.35	0.31	155.62	112.89	142.45	153.56
4	50.12	57.30	52.45	49.07	63.00	68.50	65.00	70.00	0.36	0.30	0.34	0.34	153.17	146.65	150.92	154.93
5	38.37	54.47	45.55	48.39	73.00	79.00	76.00	79.00	0.26	0.19	0.22	0.26	78.99	83.92	82.26	109.92
6	69.25	78.06	66.99	77.90	71.00	76.00	66.00	88.50	0.28	0.22	0.33	0.16	163.22	148.55	187.66	116.85
7	53.89	56.91	51.13	56.95	63.00	66.00	56.00	72.00	0.36	0.33	0.43	0.32	163.84	157.61	187.33	169.75
8	56.87	63.49	52.56	64.95	65.00	71.50	66.00	82.00	0.34	0.27	0.33	0.23	162.83	144.93	146.17	135.53
9	62.03	59.04	56.65	68.81	68.00	77.00	64.00	73.00	0.31	0.21	0.35	0.32	154.81	101.43	160.64	191.44
10	56.42	66.58	57.20	63.29	69.00	78.50	61.00	90.00	0.30	0.20	0.38	0.15	135.60	105.60	176.05	83.77

mean	54.86	60.99	52.31	59.97	67.30	73.90	65.30	78.55	0.32	0.25	0.34	0.26	144.51	123.89	147.85	139.26
std	8.22	8.03	6.83	9.13	3.62	4.65	5.10	7.31	0.04	0.05	0.05	0.07	25.50	24.78	33.29	34.10

std = standard deviation

**Supplementary Table 2.** The change in end-tidal CO<sub>2</sub> (pEtCO<sub>2</sub>), global cerebral blood flow (CBF), venous oxygenation (Y<sub>v</sub>), oxygen extraction fraction (OEF), and cerebral metabolic rate of oxygen (CMRO<sub>2</sub>) for the 'CO<sub>2</sub> in air' and carbogen breathing conditions with respect to the room air breathing condition for all subjects.

subj. nr	change in pEtCO <sub>2</sub>		change in CBF				change in Y <sub>v</sub>		change in OEF				change in CMRO <sub>2</sub>			
	ΔpEtCO <sub>2</sub> (mmHg)		ΔCBF (ml/100g/min)		ΔCBF (%)		ΔY <sub>v</sub> (%)†		ΔOEF		ΔOEF (%)		ΔCMRO <sub>2</sub> (μmol/100g/min)		ΔCMRO <sub>2</sub> (%)	
	CO <sub>2</sub> in air	carbogen	CO <sub>2</sub> in air	carbogen	CO <sub>2</sub> in air	carbogen	CO <sub>2</sub> in air	carbogen	CO <sub>2</sub> in air	carbogen	CO <sub>2</sub> in air	carbogen	CO <sub>2</sub> in air	carbogen	CO <sub>2</sub> in air	carbogen
1	3.00	4.20	8.31	14.81	12.28	25.65	11.39	19.53	-0.10	-0.10	-50.28	-51.63	-34.62	-3.97	-24.20	-3.56
2	5.70	1.00	3.99	9.88	7.22	16.61	4.23	8.84	-0.03	-0.01	-11.78	-2.69	-4.99	35.88	-3.73	26.88
3	2.00	0.80	0.10	5.10	0.20	9.60	13.10	12.33	-0.10	-0.04	-38.06	-11.33	-42.73	11.12	-27.46	7.80
4	5.10	3.70	7.19	-3.39	12.54	-6.90	8.03	7.14	-0.06	0.00	-19.27	1.10	-6.52	4.01	-4.26	2.66
5	3.30	5.20	16.10	2.84	29.55	5.86	7.59	3.80	-0.06	0.03	-33.50	13.39	4.93	27.67	6.24	33.64
6	4.30	4.20	8.81	10.91	11.29	14.00	6.58	25.42	-0.05	-0.17	-23.72	-102.39	-14.66	-70.80	-8.98	-37.73
7	2.60	6.60	3.01	5.82	5.30	10.21	4.55	22.22	-0.03	-0.11	-9.69	-33.45	-6.23	-17.57	-3.80	-9.38
8	3.00	5.80	6.62	12.39	10.43	19.07	9.09	19.51	-0.07	-0.10	-25.34	-44.77	-17.90	-10.63	-10.99	-7.28
9	7.40	7.00	-2.99	12.16	-5.07	17.67	11.69	12.33	-0.10	-0.03	-44.98	-10.82	-53.37	30.81	-34.48	19.18
10	5.50	6.00	10.17	6.09	15.27	9.62	12.10	32.22	-0.10	-0.23	-51.34	-153.09	-30.01	-92.28	-22.13	-52.42
mean	4.19	4.45	6.13	7.66	9.90	12.14	8.84	16.33	-0.07	-0.08	-30.80	-39.57	-20.61	-8.58	-13.38	-2.02
std	1.70	2.16	5.40	5.45	9.29	8.84	3.17	8.94	0.03	0.08	15.21	52.16	18.83	42.65	12.98	27.03

pEtCO<sub>2</sub> = end-tidal partial pressure of CO<sub>2</sub>, CBF = global cerebral blood flow, Y<sub>v</sub> = venous blood oxygenation, OEF = oxygen extraction fraction, CMRO<sub>2</sub> = cerebral metabolic rate of oxygen, std = standard deviation, †note this is the fractional change in percentage in Y<sub>v</sub>, i.e. not percentage points.

## References

1. Buxton RB, Frank LR, Wong EC, et al. A general kinetic model for quantitative perfusion imaging with arterial spin labeling. *Magnetic Resonance in Medicine* 1998; 40: 383–396.
2. Rooney WD, Johnson G, Li X, et al. Magnetic field and tissue dependencies of human brain longitudinal  $^1\text{H}_2\text{O}$  relaxation in vivo. *Magnetic Resonance in Medicine* 2007; 57: 308–318.
3. Juttukonda MR, Li B, Almaktooum R, et al. Characterizing cerebral hemodynamics across the adult lifespan with arterial spin labeling MRI data from the Human Connectome Project-Aging. *NeuroImage*; 230. Epub ahead of print 2021. DOI: 10.1016/j.neuroimage.2021.117807.
4. Ma Y, Berman AJL, Pike GB. The effect of dissolved oxygen on the relaxation rates of blood plasma: Implications for hyperoxia calibrated BOLD. *Magnetic Resonance in Medicine* 2016; 76: 1905–1911.
5. Siero JCW, Strother MK, Faraco CC, et al. In vivo quantification of hyperoxic arterial blood water T1. *NMR in Biomedicine* 2015; 28: 1518–1525.
6. Lu H, Clingman C, Golay X, et al. Determining the longitudinal relaxation time (T1) of blood at 3.0 tesla. *Magnetic Resonance in Medicine* 2004; 52: 679–682.
7. Pilkinton DT, Hiraki T, Detre JA, et al. Absolute cerebral blood flow quantification with pulsed arterial spin labeling during hyperoxia corrected with the simultaneous measurement of the longitudinal relaxation time of arterial blood. *Magnetic Resonance in Medicine* 2012; 67: 1556–1565.
8. Li W, Grgac K, Huang A, et al. Quantitative theory for the longitudinal relaxation time of blood water. *Magnetic Resonance in Medicine* 2016; 76: 270–281.